

Longitudinal mode of spin fluctuations in iron-based superconductors

Qiang Zhang¹ and Jiangping Hu^{1,2,3,*}

¹*Beijing National Laboratory for Condensed Matter Physics,
and Institute of Physics, Chinese Academy of Sciences, Beijing 100190, China*

²*Collaborative Innovation Center of Quantum Matter, Beijing, China*

³*Kavli Institute of Theoretical Sciences, University of Chinese Academy of Sciences, Beijing 100049, China*

Iron-based superconductors can exhibit different magnetic ground states and are in a critical magnetic region where frustrated magnetic interactions strongly compete with each other. Here we investigate the longitudinal modes of spin fluctuations in an unified effective magnetic model for iron-based superconductors. We focus on the collinear antiferromagnetic phase and calculate the behavior of the longitudinal mode when different phase boundaries are approached. The results can help to determine the nature of the magnetic fluctuations in iron-based superconductors.

I. INTRODUCTION

Iron-based superconductors have very rich magnetic properties^{1,2}. They exhibit many intriguing magnetically ordered ground states, including stripe-like collinear antiferromagnetic (CAF) state³, checkerboard-like antiferromagnetic (AFM) state⁴, bi-collinear antiferromagnetic (BCAF) state⁵, staggered dimer (DI)⁶ state and some incommensurate (IC) states. The superconductivity appears to be linked to the magnetism, in particular, the CAF state⁷. The origin of these magnetic states thus has been one of central focus in this field.

Although both itinerant and local spin theories are reasonably successful in explaining magnetic properties of some certain families of iron-based superconductors, it has been crystal clear that the magnetism is a hybrid with dual characters from both itinerant electrons and local spin moments^{8,9}. However, microscopically, the system can not be simply described by a Kondo lattice type of model because it is very difficult to separate itinerant electrons from localized ones.

A reasonable strategy is to seek an effective magnetic model. With the existence of local magnetic moments, we can still focus on the effective interactions between these local moments by integrating out of itinerant electrons to obtain a minimum magnetic effective model by keeping those Heisenberg-type leading interactions with the shortest distances. This approach has yielded a successful effective model, the $J_1 - J_2 - J_3 - K$ model⁸⁻¹⁵. In this model, the nearest neighbor (NN) magnetic interaction J_1 and the next NN one J_2 arise mainly through local magnetic direct exchange and magnetic superexchange mechanisms. The third NN interaction J_3 and the quartic interaction K indicate the existence of the strong couplings to itinerant electrons. The phase diagram of the model has been studied extensively^{8,9}. The mean-field results of the model can account for most magnetic phases and low energy magnetic excitations observed experimentally in iron-based superconductors⁸ except some recently observed orders in very specific situations such as the double-**Q** orders^{16,17}. The magnetism in the effective model is extremely frustrated due to the strong competition among J_1 , J_2 and J_3 , which is also consis-

tent with the fact that the long range magnetic order is absent in some iron-based superconductors.

In a model based on local magnetic moments, the spin waves (SW) are the low energy excitations in a given magnetically ordered state. The SW are the transverse modes, namely the magnetic fluctuations perpendicular to the direction of the ordered moment. The longitudinal modes (LM), which are parallel to the ordered moments, are gapped out as Higgs mode. However, if there are several competing magnetic states, the LM can start to appear at low energy even at zero temperature. Therefore, the gaps of the LM (Higgs mass) can provide us important information about the degree of magnetic frustration¹⁸⁻²⁰.

Recently, several polarized neutron scattering experiments have been carried out in the CAF state of iron-based superconductors¹⁹⁻²³. The gapped LM have been observed. The observed gaps of these LM are much lower than the band width of spin excitations. Thus, these measurements suggest the existence of strong magnetic frustration in the materials. The materials may be close to a quantum critical point or are located close to a spin liquid region^{24,25}.

Longitudinal excitations was viewed as support for itinerant magnetism^{19,26,27}. In this paper, we use a new method to analytically calculate the LM from the effective exchange model, in particular, in the parameter region of the CAF state near the phase boundary. We find that the LM become visible at low energy close to the phase boundary and they have different dispersion relations from the transverse SW modes. They disperse very rapidly along the antiferromagnetic direction and have very little dispersion along the FM direction in the CAF phase. This feature is absent in other magnetically ordered states so that it is unique for the CAF state. Therefore, our results suggest that the measurement of the LM in a paramagnetic state that has a finite magnetic correlation length can be used to determine how the system is close to the CAF state.

II. THE $J_1 - J_2 - J_3 - K$ MODEL

The $J_1 - J_2 - J_3 - K$ model^{8,9} is described by

$$H = \sum_{\langle i,j \rangle} J_1 \vec{S}_i \cdot \vec{S}_j + \sum_{\langle\langle i,j \rangle\rangle} J_2 \vec{S}_i \cdot \vec{S}_j + \sum_{\langle\langle\langle i,j \rangle\rangle\rangle} J_3 \vec{S}_i \cdot \vec{S}_j - \sum_{\langle i,j \rangle} K (\vec{S}_i \cdot \vec{S}_j)^2, \quad (1)$$

which includes the nearest (J_1), second (J_2) and third (J_3) nearest neighbor Heisenberg interactions and $K (> 0)$ quartic term^{12,28}. Various magnetic phases can be classified in Fig.1. We will focus on the LM in the CAF phase and the behavior of approaching the phase boundaries.

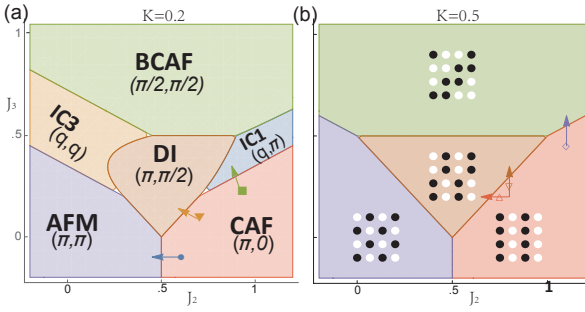


FIG. 1: Various classical states for $K = 0.2$ (a) and $K = 0.5$ (b) in the unit of J_1 ($s = 1$) as classified in literatures^{8,9}. For small K in (a), the incommensurate phases insert in the middle of the parameter space. For bigger K (b), the commensurate phases expand to cover the whole parameter space. The black-white dots represent the up-down spins in real space for commensurate phases. The filled inverted triangle marks FeSe at 9 GPa ⁹ and the arrows indicate the paths approaching the phase boundaries.

This Hamiltonian can be solved within the standard spin wave (*Holstein-Primakov*) theory. Starting from the above depicted classical ground state, we rotate the down spins and then represent the spins \vec{S}_i with magnons a_i, a_i^\dagger :

$$\begin{aligned} S_i^z &\rightarrow -S_i^z, & S_i^\pm &\rightarrow -S_i^\mp, \\ S_i^z &= s - a_i^\dagger a_i, & S_i^+ (S_i^-) &= \chi a_i (a_i^\dagger \chi), \end{aligned} \quad (2)$$

with $\chi = \sqrt{2s - a_i^\dagger a_i}$. When the local environment for each spin is not identical, there are several spins in one magnetic cell and the site $i = \{c, a\}$ with $c = 1, \dots, N'$ counting for the cells and $a = 1, \dots, n$ for the magnon types. Up to two-magnon operators (we would omit the vector notation for position and momentum), the approximate Hamiltonian in momentum space is

$$H \approx \sum_k \frac{1}{2} s \Psi_k^\dagger H_k \Psi_{-k} - \sum_k \frac{1}{2} s \text{Tr}(H_k) + E_0, \quad (3)$$

with H_k the $2n \times 2n$ matrix, E_0 the classical ground state energy and $\Psi_k^\dagger = (\mathbf{a}_k^\dagger, \mathbf{a}_{-k}^T)$, where \mathbf{a}_k is a column

collection of magnon annihilators and \mathbf{a}_k^T is the matrix transpose. As derived in the appendix.(A), this Hamiltonian can be diagonalized by *Bogoliubov* transformation²⁹ and the SW spectra ϵ_{nk} are the eigenvalues of $\sigma_{zn} H_k$. Here

$$H_k = \begin{pmatrix} \omega_k & \gamma_k \\ \gamma_k^\dagger & \omega_{-k}^T \end{pmatrix}, \quad \sigma_{zn} = \begin{pmatrix} I_n & 0 \\ 0 & -I_n \end{pmatrix} \quad (4)$$

with I_n the $n \times n$ identical matrix and $\omega_k = \omega_k^\dagger = \omega_{-k}^T$, $\gamma_k = \gamma_{-k}^T = \gamma_k^\dagger$. When $n = 1$, it is easy to find $\epsilon_k = s\sqrt{\omega_k^2 - \gamma_k^2}$. This SW spectrum is generally gapless at the order momentum as the *Goldstone* mode. Coupling anisotropy can interpret the observed gap¹⁹. We would shift the Heisenberg to *XXZ* coupling $\vec{S}_i \cdot \vec{S}_j = S_i^x S_j^x + S_i^y S_j^y + A S_i^z S_j^z$, with $A = 1 + \delta_a$. This positive δ_a will pick up the easy axis and speed up the numerical calculations.

A. The Longitudinal Mode

In quantum antiferromagnet, the longitudinal modes are the amplitude fluctuation of the ordered moments $\langle S^z \rangle$, essentially, magnon density. Different from the itinerant approach²⁷ and nonlinear- σ model^{18,26}, LM can also be viewed as two magnon resonance³⁰ or magnon density wave³¹ in Holstein-Primakov theory. Following Feynman's approach to the helium superfluid³², the LM can be defined as:

$$|L_q\rangle \equiv \frac{1}{\sqrt{N}} \sum_i e^{iq \cdot \vec{r}_i} S_i^z |0\rangle = \frac{1}{\sqrt{N}} \sum_k a_k^\dagger a_{k+q} |0\rangle. \quad (5)$$

With respect to the ground state, the LM has the spectrum:

$$E(q) = \frac{N(q)}{S(q)}, \quad (6)$$

with $N(q) \equiv \langle L_q | H | L_q \rangle$ and $S(q) \equiv \langle L_q | L_q \rangle$ the structure factor. Separating the Hamiltonian by neighborhood (\vec{m}) coupling: $H = \sum_m H_m + \sum_m H_m^K$, we have

$$N(q) = \sum_m N_m(q) + \sum_m N_m^K(q) \quad (7)$$

with (dependent on whether the \vec{m} neighbor spins are anti-parallel or parallel (AP/P))

$$N_m(q) = \begin{cases} \frac{J_m}{2n} \sum_a (\cos(qm) + 1) \Pi_{m+}, & AP \\ \frac{J_m}{2n} \sum_a (\cos(qm) - 1) \Pi_{m-}, & P \end{cases} \quad (8)$$

$$N_m^K(q) = \begin{cases} \frac{Ks^2}{n} \sum_a (\cos(qm) + 1) \Pi_{m+}^K, & AP \\ -\frac{Ks^2}{n} \sum_a (\cos(qm) - 1) \Pi_{m-}^K, & P \end{cases} \quad (9)$$

where \sum_a sums over different magnon types and the correlation function Π 's are (see appendix.A)

$$\Pi_{m+} = 2s\Delta_{ab} - \Delta_{ab}(\rho_{aa} + \rho_{bb}) - \rho_{ab}(\Delta_{aa} + \Delta_{bb}),$$

$$\begin{aligned}
\Pi_{m-} &= 2s\rho_{ab} - \rho_{ab}(\rho_{aa} + \rho_{bb}) - \Delta_{ab}(\Delta_{aa} + \Delta_{bb}), \\
\Pi_{m+}^K &= 8\Delta_{ab}^2 + 4\Delta_{aa}\Delta_{bb} + A(2(s-1)\rho_{ab} \\
&\quad - 5\rho_{ab}(\rho_{aa} + \rho_{bb}) - 5/2\Delta_{ab}(\Delta_{aa} + \Delta_{bb})), (10) \\
\Pi_{m-}^K &= 8\rho_{ab}^2 + 4\Delta_{aa}\Delta_{bb} + A(2(s-1)\Delta_{ab} \\
&\quad - 5\Delta_{ab}(\rho_{aa} + \rho_{bb}) - 5/2\rho_{ab}(\Delta_{aa} + \Delta_{bb})).
\end{aligned}$$

Here $\rho_{ab}(m) \equiv \langle a_i^\dagger b_{i+m} \rangle$, $\Delta_{ab}(m) \equiv \langle a_i b_{i+m} \rangle$ are the correlations of type a, b magnon at site $i, i+m$. We have omitted the neighborhood (m) to simplify the notation. The quartic K term modifies the exchange J by $\pm 2AKs^2$ at the first order of large s . The $n \times n$ correlation matrices in momentum space ρ_k , Δ_k are the Fourier transformation of $\rho(m)$, $\Delta(m)$. The structure factor is

$$S(q) = \frac{1}{n} \text{Tr} \left[\rho(0) + \frac{1}{N'} \sum_k (\rho_k \rho_{k+q} + \Delta_k \Delta_{k+q}) \right]. \quad (11)$$

In the case of one type magnon, the SW spectrum and the correlators can be solved analytically:

$$\begin{aligned}
\epsilon_k &= s\sqrt{\omega_k^2 - \gamma_k^2}, \\
\rho_k &= (\sqrt{\omega_k^2 / (\omega_k^2 - \gamma_k^2)} - 1)/2, \\
\Delta_k &= -\gamma_k / (2\sqrt{\omega_k^2 - \gamma_k^2}).
\end{aligned} \quad (12)$$

B. The CAF Phase

The CAF phase with ordered momentum $\mathbf{Q} = X = (\pi, 0)$ is an example of the exactly solvable case of Eq.(12) with

$$\begin{aligned}
\omega_k &= 2(J_1 - 2AKs^2) \cos k_y + 4AJ_2 + 8A^2Ks^2 \\
&\quad + 2J_3(\cos 2k_x + \cos 2k_y - 2A), \\
\gamma_k &= -2(J_1 + 2AKs^2 + 2J_2 \cos k_y) \cos k_x.
\end{aligned} \quad (13)$$

The spectra of SW and LM for FeSe at 9 GPa⁹ are depicted in Fig.2, in the unit of J_1s (51.1 meV). The Goldstone modes appear at Γ and \mathbf{Q} in the SW spectrum Fig.2(a). In our calculation, the anisotropic exchange opens a tiny gap $0.07J_1s$ ($\sim \sqrt{\delta_a}$). This is often introduced to explain the observed anisotropic gap in the transverse modes¹⁹. In totally isotropic case ($\delta_a = K = 0$), it would be gapless at all high symmetry points $YMX\Gamma$ as one can see from Eq.(12). Zooming into \mathbf{Q} , the SW has oval-shape equal energy line as seen from the 3D view in Fig.2(c) which has been measured experimentally.

The LM spectrum is depicted in Fig.2(b). It has a deep valley structure along the $k_x = \pi$ line. The dispersion is flat in $(\pi, \pm\delta_q)$ direction, but it is steep in $(\pi \pm \delta_q, 0)$ as shown in Fig.2(b,d). The valley structure is manifested in Fig.2(d). It is interesting to point out that at $\mathbf{Q} = (\pi, 0)$, the structure factor $S(\mathbf{Q}) = 0$. This is protected by the symmetry $\gamma_{k+Q} = -\gamma_k$, not an issue of approximation. The coupling in c axis can break this symmetry, resulting in a well-defined LM. Indeed, J_c is important for the

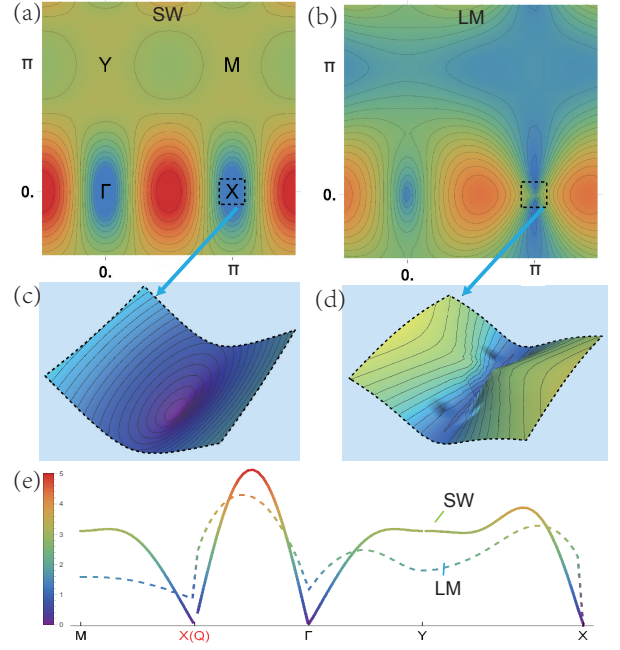


FIG. 2: The spectra of SW and LM for CAF phase. Here we used the parameters for *FeSe* at 9GPa⁹: $K = 0.2$, $J_2 = 0.69$, $J_3 = 0.09$. $A = 1.0001$ is used to slightly gap the SW Goldstone modes and speed up the calculation. The color (bar in (e)) marks the energy for SW (a,c) and LM (b,d). ΓXMY in (a) mark the high symmetry points. The 3D dispersion (c,d) are taken from the dashed square region ($\pi \pm 0.1\pi, \pm 0.1\pi$). The SW is gapless ($0.07J_1$) and slightly anisotropic with oval-shape equal-energy slice and that the LM is gapped ($0.87J_1$) and strongly anisotropic with open equal-energy curve bending outward. The projected dispersion (e) clearly shows Goldstone mode and Higgs mode at $X(\mathbf{Q})$.

occurrence of long range magnetic order. Yet, for numerical consideration, the longitudinal gap can be obtained from the nearby region since Eq.(6) is a smooth function except at \mathbf{Q} .

The dispersion along some high symmetry directions are shown in Fig.2(e). As expected, the transverse mode converges to almost zero and its linear dispersion shows slight anisotropy at \mathbf{Q} . The LM at this point is gapped and strongly anisotropic. The dispersion is flat in q_y (XM) direction and sharp in q_x ($X\Gamma$) direction. The calculated longitudinal gap $\Delta = 0.87J_1s = 44.5$ meV, which is not measured yet.

As approaching the phases boundaries, the order parameter would be softened due to the competition among various magnetic orders³⁰ and the LM would appear in low energy as frustration arises. The longitudinal gap Δ is depicted in Fig.3 as approaching the phase boundaries. The gap is taken as the limit from the flat k_y direction. The gap Δ drops to zero near the phases boundaries, appearing as low energy excitation in the neutron scattering experiment. We also noticed that the gaps of the three empty markers ($K=0.5$), as routes

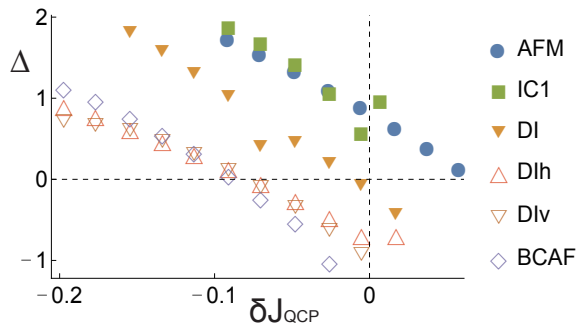


FIG. 3: The longitudinal gaps Δ as functions of the distance δJ_{QCP} to various neighbor phases. The approaching paths are marked by color arrows in Fig.1(a). The empty markers ($K = 0.5$) manifest smaller gaps, possibly indicating stronger frustration compared with filled markers ($K = 0.2$).

approaching BCAF, DI-horizontally and DI-vertically respectively, drop faster to zero in front of the boundaries, as a possible sign of stronger frustration. No big difference is found for the paths approaching the DI phases horizontally (varying J_2) and vertically (varying J_3). Thus in this effective model, localized exchange and itinerant coupling equivalently contribute to frustration to hold LM.

Adjust to the models and parameters in Ref.¹⁹, a 53 meV longitudinal gap can be obtained with our calculation, comparing with the observed value $25 \sim 30$ meV. This result is very reasonable. As fluctuation effect in the vicinity of critical region is underestimated in our method, the gap in our calculation should be larger than the true gap. For more accurate quantitative result, the higher order correction has to be considered.

C. Other Magnetic Phase

Similar work can be done for various magnetic phases represented in Fig.1, following the method generally described in Appendix.(A). The J_1 dominated AF state with $\mathbf{Q}' = M = (\pi, \pi)$ is another example of exactly solvable case. Its SW the LM along the high symmetry points are in Fig.4. Similar to the CAF phase, the SW is gapless and the LM is gapped at \mathbf{Q}' . The magnetic environment is C_4 symmetric and both the SW and LM dispersion are isotropic. Approaching to the phases boundaries, the longitudinal gaps also decreases to appear as low excitations due to phases competition. The LM are always more sensitive to the quantum frustration. Near the quantum critical point, the interaction among magnons in LM breaks the ground state.

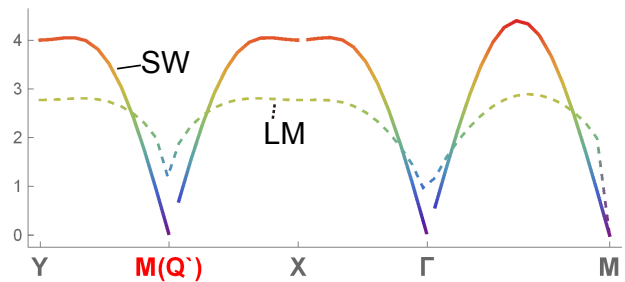


FIG. 4: The spectra for SW and LM for AF state along the high symmetry points with parameters $K = 0.2$, $J_2 = 0.2$, $J_3 = 0.05$ and $A = 1.0001$. The SW gap at \mathbf{Q}' is zero and LM $\Delta = 1.20$ in the unit of $J_1 s$.

III. DISCUSSION AND SUMMARY

Recently, the inelastic neutron scattering experiments have already measured the LM in iron-based superconducting materials^{19,20,33-35}. These results are typically considered as evidence to support pure itinerant magnetism in these materials^{19,26,27}. However, as argued in literature⁸, a pure itinerant magnetism can not explain all the observed magnetic properties in iron-based superconductors. According to our calculation, LM can also emerge from the effective exchange model.

Combining with the experimental results, our results strongly support that iron-based superconductors are strongly frustrated magnetic systems in a vicinity to many different magnetic phases. In particular, the CAF order is very close to quantum critical transitions to other magnetic orders. The nature of the frustration stems from the competitions between short range local magnetic exchange couplings and other effective magnetic interactions through couplings with itinerant electrons.

In summary, we derived the longitudinal excitation for the general $J_1 - J_2 - J_3 - K$ magnetic model. Specifically, the analytic solution in the CAF state is given. The dispersion of the LM in the CAF state near the quantum critical point is very different from the transverse SW modes.

Acknowledgement: the work is supported by the Ministry of Science and Technology of China 973 program(Grant No. 2015CB921300), National Science Foundation of China (Grant No. NSFC-11334012, No. NSFC-11534014), the Strategic Priority Research Program of CAS (Grant No. XDB07000000) and the International Young Scientist Fellowship of Institute of Physics CAS (Grant No.2017002).

Appendix A: Derivation

1. Spin Wave spectrum

The magnon satisfies the bosonic commute relation:

$$\Psi_k \Psi_q^\dagger - ((\Psi_q^\dagger)^T \Psi_k^T)^T = \delta_{kq} \sigma_{zn}. \quad (\text{A1})$$

With the help of *Bogoliubov* transformation $\Psi_k = T_k \Phi_k$, where $\Phi_k^\dagger = (\mathbf{d}_k^\dagger, \mathbf{d}_{-k}^T)$, the Hamiltonian can be diagonalized as $T_k^\dagger H_k T_k = \sigma_{zn} \Lambda_k$, when the transformation matrix satisfy

$$\begin{aligned} \sigma_{zn} &= T_k \sigma_{zn} T_k^\dagger, \\ \Lambda_k &= T_k^{-1} (\sigma_{zn} H_k) T_k, \end{aligned} \quad (\text{A2})$$

where Λ_k is the diagonalized matrix of $\sigma_{zn} H_k$ by similarity transformation and T_k is the Bogoliubov matrix²⁹:

$$T_k = \begin{pmatrix} \mu_k & \nu_k \\ \nu_{-k}^* & \mu_{-k}^* \end{pmatrix}, \quad (\text{A3})$$

where μ_k, ν_k are the $n \times n$ *coherent phase* matrices. One can collect the eigenvectors of matrix $\sigma_{zn} H_k$ and then normalize them by equation.(A2). It is proven that for the eigenvalue ϵ_k with eigenvector \mathbf{v}_k , there exists a dual eigenvalue $-\epsilon_{-k}^*$ with eigenvector $\sigma_{zn} \mathbf{v}_{-k}^*$. Thus by properly order the eigenvalues and adjust the relative phases, this T_k is the Bogoliubov matrix to diagonalize the Hamiltonian via congruence transformation. In algorithm, there could be phase freedom for those eigenvectors, making the matrix non-Bogoliubov, i.e. $T \rightarrow T e^{i\Theta}$ with $\Theta = \text{diag}\{\theta_1, \dots, \theta_{2n}\}$ the phases matrix. It's easy to remove those phases and, moreover, this phase freedom does not affect the SW spectra and the LM.

In linear SW theory, the Hamiltonian matrix elements are the Fourier transformation of the neighborhood interaction in real space, so $\omega_k, \gamma_k, \epsilon_k, \mu_k, \nu_k$ all satisfy $f^*(k) = f(-k)$ and the diagonalized Hamiltonian $\sigma_{zn} \Lambda_k$ is real and doubly degenerate.

2. Longitudinal Spectrum

The essence of calculating the ground state expectation of the commutators $N_m(q)$ and $N_m^K(q)$ in equ.(7) is to calculate the correlation of spins, up to second $\langle SS \rangle$ and forth order $\langle SSSS \rangle$. Define the magnon correlators first:

$$\langle \Psi_k \Psi_q^\dagger \rangle = \begin{pmatrix} \mu_k \mu_k^\dagger & \mu_k \nu_{-k}^T \\ \nu_{-k}^* \mu_k^\dagger & \nu_{-k}^* \nu_{-k}^T \end{pmatrix} \delta_{kq} = \begin{pmatrix} \rho_k^T + 1 & \Delta_{-k} \\ \Delta_{-k}^\dagger & \rho_{-k} \end{pmatrix} \delta_{kq}.$$

It is easy to see $\rho_k^\dagger = \rho_k$ and $\Delta_k = \Delta_{-k}^T$. In linear spin theory, $f(-k) = f^*(k)$ also works for ρ_k and Δ_k . The real space correlations

$$\rho(m) \equiv \langle \mathbf{a}_l^\dagger \mathbf{a}_{l+m}^T \rangle = \frac{1}{N^l} \sum_k e^{-ikm} \rho_k, \quad (\text{A4})$$

$$\Delta(m) \equiv \langle \mathbf{a}_l \mathbf{a}_{l+m}^T \rangle = \frac{1}{N^l} \sum_k e^{-ikm} \Delta_k \quad (\text{A5})$$

satisfy $\rho^*(m) = \rho^\dagger(-m) = \rho(m)$ and $\Delta^*(m) = \Delta^\dagger(-m) = \Delta(m)$. Thus the correlation among different magnons is the elements of the correlation matrices $\rho(m)$ and $\Delta(m)$:

$$\begin{aligned} \langle a_l^\dagger b_{l+m} \rangle &= \rho_{ab}(m) = \langle a_l b_{l+m}^\dagger \rangle - \delta_{m0}, \\ \langle a_l b_{l+m} \rangle &= \Delta_{ab}(m) = \langle a_l^\dagger b_{l+m}^\dagger \rangle. \end{aligned} \quad (\text{A6})$$

For higher (even) operators correlation, thereafter, the *contraction rules* can be concluded $\langle c_1 c_2 \dots c_{2n-1} c_{2n} \rangle$ ($c_i = a_i, a_i^\dagger$):

1. Put the c 's operators in pairs, all possible combinations;
2. Refer to the matrix element of $\rho(m)$ and $\Delta(m)$, write all the operator pairs as two-operator correlation functions in real space.

Referring this contraction rule, the following four operators (and their conjugate) correlation is needed:

$$\begin{aligned} \langle a_i b_j a_i b_j \rangle &= 2\Delta_{ab}^2 + \Delta_{aa} \Delta_{bb}, \\ \langle a_i b_j^\dagger a_i b_j^\dagger \rangle &= 2\rho_{ab}^2 + \Delta_{aa} \Delta_{bb}, \\ \langle a_i^\dagger b_j^\dagger a_i^\dagger a_j \rangle &= 2\rho_{aa} \Delta_{ab} + \rho_{ab} \Delta_{aa}, \\ \langle a_i b_j^\dagger b_j^\dagger b_j \rangle &= 2\rho_{bb} \rho_{ab} + \Delta_{ab} \Delta_{bb}. \end{aligned} \quad (\text{A7})$$

We omit the variables $(j-i)$ within ρ_{ab}, Δ_{ab} for convenience. Relevant to the LM up to the four operators correlation, for $N_m(q)$, we need to estimate :

$$\begin{aligned} \langle S_i^\dagger S_j^- \rangle &= 2s\rho_{ab} - \rho_{ab}(\rho_{aa} + \rho_{bb}) - \Delta_{ab}(\Delta_{aa} + \Delta_{bb})/2, \\ \langle S_i^- S_j^- \rangle &= 2s\Delta_{ab} - \Delta_{ab}(\rho_{aa} + \rho_{bb}) - \rho_{ab}(\Delta_{aa} + \Delta_{bb})/2, \end{aligned}$$

and in the quartic term $N_m^K(q)$

$$\begin{aligned} \langle S_i^- S_j^- S_i^- S_j^- \rangle &\approx (2s)^2 (2\Delta_{ab}^2 + \Delta_{aa} \Delta_{bb}), \\ \langle S_i^\dagger S_j^- S_i^\dagger S_j^- \rangle &\approx (2s)^2 (2\rho_{ab}^2 + \Delta_{aa} \Delta_{bb}), \\ \langle S_i^\dagger S_j^- S_i^z S_j^z \rangle &\approx s^2 (2(s-1)\rho_{ab} - 5\rho_{ab}(\rho_{aa} + \rho_{bb}) \\ &\quad - 5/2\Delta_{ab}(\Delta_{aa} + \Delta_{bb})), \\ \langle S_i^\dagger S_j^z S_i^z S_j^z \rangle &\approx s^2 (2(s-2)\Delta_{ab} - 5\Delta_{ab}(\rho_{aa} + \rho_{bb}) \\ &\quad - 5/2\rho_{ab}(\Delta_{aa} + \Delta_{bb})), \end{aligned}$$

With the above correlators derived, the correlation function Π 's in $N(q)$ can be obtained.

* Electronic address: jphu@iphy.ac.cn

¹ P. Dai, J. Hu, and E. Dagotto, Nature Physics **8**, 709

(2012).

² P. Dai, Rev. Mod. Phys. **87**, 855 (2015), URL <http://>

- link.aps.org/doi/10.1103/RevModPhys.87.855.
- ³ C. de La Cruz, Q. Huang, J. Lynn, J. Li, W. Ratcliff II, J. L. Zarestky, H. Mook, G. Chen, J. Luo, N. Wang, et al., *nature* **453**, 899 (2008).
 - ⁴ K. Marty, A. D. Christianson, C. H. Wang, M. Matsuda, H. Cao, L. H. VanBebber, J. L. Zarestky, D. J. Singh, A. S. Sefat, and M. D. Lumsden, *Phys. Rev. B* **83**, 060509 (2011), URL <http://link.aps.org/doi/10.1103/PhysRevB.83.060509>.
 - ⁵ W. Bao, Y. Qiu, Q. Huang, M. A. Green, P. Zajdel, M. R. Fitzsimmons, M. Zhernenkov, S. Chang, M. Fang, B. Qian, et al., *Phys. Rev. Lett.* **102**, 247001 (2009), URL <http://link.aps.org/doi/10.1103/PhysRevLett.102.247001>.
 - ⁶ H.-Y. Cao, S. Chen, H. Xiang, and X.-G. Gong, *Physical Review B* **91**, 020504 (2015).
 - ⁷ I. I. Mazin, D. J. Singh, M. D. Johannes, and M. H. Du, *Phys. Rev. Lett.* **101**, 057003 (2008), URL <http://link.aps.org/doi/10.1103/PhysRevLett.101.057003>.
 - ⁸ J. Hu, B. Xu, W. Liu, N.-N. Hao, and Y. Wang, *Phys. Rev. B* **85**, 144403 (2012), URL <http://link.aps.org/doi/10.1103/PhysRevB.85.144403>.
 - ⁹ J. Glasbrenner, I. Mazin, H. O. Jeschke, P. Hirschfeld, R. Fernandes, and R. Valentí, *Nature Physics* **11**, 953 (2015).
 - ¹⁰ C. Fang, B. A. Bernevig, and J. Hu, *EPL (Europhysics Letters)* **86**, 67005 (2009).
 - ¹¹ C. Fang, H. Yao, W.-F. Tsai, J. Hu, and S. A. Kivelson, *Physical Review B* **77**, 224509 (2008).
 - ¹² A. N. Yaresko, G.-Q. Liu, V. N. Antonov, and O. K. Andersen, *Phys. Rev. B* **79**, 144421 (2009), URL <http://link.aps.org/doi/10.1103/PhysRevB.79.144421>.
 - ¹³ A. L. Wysocki, K. D. Belashchenko, and V. P. Antropov, *Nature Physics* **7**, 485 (2011).
 - ¹⁴ J. K. Glasbrenner, J. P. Velev, and I. I. Mazin, *Phys. Rev. B* **89**, 064509 (2014), URL <http://link.aps.org/doi/10.1103/PhysRevB.89.064509>.
 - ¹⁵ M. Wang, C. Fang, D.-X. Yao, G. Tan, L. W. Harriger, Y. Song, T. Netherton, C. Zhang, M. Wang, M. B. Stone, et al., *Nature communications* **2**, 580 (2011).
 - ¹⁶ G. Giovannetti, C. Ortix, M. Marsman, M. Capone, J. Van Den Brink, and J. Lorenzana, *Nature communications* **2**, 398 (2011).
 - ¹⁷ M. Hoyer, R. M. Fernandes, A. Levchenko, and J. Schmalian, *Phys. Rev. B* **93**, 144414 (2016), URL <https://link.aps.org/doi/10.1103/PhysRevB.93.144414>.
 - ¹⁸ F. D. M. Haldane, *Phys. Rev. Lett.* **50**, 1153 (1983), URL <http://link.aps.org/doi/10.1103/PhysRevLett.50.1153>.
 - ¹⁹ C. Wang, R. Zhang, F. Wang, H. Luo, L. P. Regnault, P. Dai, and Y. Li, *Phys. Rev. X* **3**, 041036 (2013), URL <http://link.aps.org/doi/10.1103/PhysRevX.3.041036>.
 - ²⁰ H. Luo, M. Wang, C. Zhang, X. Lu, L.-P. Regnault, R. Zhang, S. Li, J. Hu, and P. Dai, *Phys. Rev. Lett.* **111**, 107006 (2013), URL <http://link.aps.org/doi/10.1103/PhysRevLett.111.107006>.
 - ²¹ N. Qureshi, P. Steffens, S. Wurmehl, S. Aswartham, B. Büchner, and M. Braden, *Phys. Rev. B* **86**, 060410 (2012), URL <http://link.aps.org/doi/10.1103/PhysRevB.86.060410>.
 - ²² Y. Song, L.-P. Regnault, C. Zhang, G. Tan, S. V. Carr, S. Chi, A. D. Christianson, T. Xiang, and P. Dai, *Phys. Rev. B* **88**, 134512 (2013), URL <http://link.aps.org/doi/10.1103/PhysRevB.88.134512>.
 - ²³ Y. Li, W. Wang, Y. Song, H. Man, X. Lu, F. Bourdarot, and P. Dai, *Phys. Rev. B* **96**, 020404 (2017), URL <https://link.aps.org/doi/10.1103/PhysRevB.96.020404>.
 - ²⁴ I. Zaliznyak, A. T. Savici, M. Lumsden, A. Tsvetlik, R. Hu, and C. Petrovic, *Proceedings of the National Academy of Sciences* **112**, 10316 (2015).
 - ²⁵ K.-J. Zhou, Y.-B. Huang, C. Monney, X. Dai, V. N. Strocov, N.-L. Wang, Z.-G. Chen, C. Zhang, P. Dai, L. Patthey, et al., *Nature communications* **4**, 1470 (2013).
 - ²⁶ Y.-Z. You, F. Yang, S.-P. Kou, and Z.-Y. Weng, *Physical Review B* **84**, 054527 (2011).
 - ²⁷ J. Knolle, I. Eremin, A. Chubukov, and R. Moessner, *Physical Review B* **81**, 140506 (2010).
 - ²⁸ P. Chandra, P. Coleman, and A. I. Larkin, *Phys. Rev. Lett.* **64**, 88 (1990), URL <http://link.aps.org/doi/10.1103/PhysRevLett.64.88>.
 - ²⁹ M.-w. Xiao, arXiv preprint arXiv:0908.0787 (2009).
 - ³⁰ I. Affleck and G. F. Wellman, *Physical Review B* **46**, 8934 (1992).
 - ³¹ Y. Xian and M. Merdan, *Journal of Physics: Conference Series* **529**, 012020 (2014), URL <http://stacks.iop.org/1742-6596/529/i=1/a=012020>.
 - ³² R. P. Feynman, *Phys. Rev.* **94**, 262 (1954), URL <http://link.aps.org/doi/10.1103/PhysRev.94.262>.
 - ³³ F. Waßer, C. Lee, K. Kihou, P. Steffens, K. Schmalzl, N. Qureshi, and M. Braden, arXiv preprint arXiv:1609.02027 (2016).
 - ³⁴ C. Zhang, Y. Song, L.-P. Regnault, Y. Su, M. Enderle, J. Kulda, G. Tan, Z. C. Sims, T. Egami, Q. Si, et al., *Physical Review B* **90**, 140502 (2014).
 - ³⁵ P. Steffens, C. H. Lee, N. Qureshi, K. Kihou, A. Iyo, H. Eisaki, and M. Braden, *Phys. Rev. Lett.* **110**, 137001 (2013), URL <http://link.aps.org/doi/10.1103/PhysRevLett.110.137001>.